Attitude Control of the Airborne Telescope SOFIA: μ-Synthesis for a Large Scaled Flexible Structure

Ulrich Schönhoff, Ascan Klein and Rainer Nordmann
Darmstadt University of Technology, Department of Mechanical Engineering, Darmstadt, Germany
`Schoenhoff@`, `Klein@` and `Nordmann@mum.tu-darmstadt.de`

Abstract

The airborne observatory SOFIA is in development with the intent to provide astronomers access to infrared wavelength unavailable from the ground. The operation of the telescope under the harsh environmental conditions in the aircraft makes the quality image stability a crucial issue. To evaluate the limits of performance that can be reached by the attitude control, a μ-synthesis optimization of the control loop is investigated during the conceptual design. A finite element model offers the most precise description of the structural dynamics of the telescope structure in this design phase and is chosen as basis for the controller design. The paper focuses on the practical aspects of robust controller design such as plant and controller reduction, weighting function selection and uncertainty modelling for flexible structures.

1 Introduction

1.1 The airborne telescope SOFIA

NASA and the German space agency DLR jointly develop the airborne telescope SOFIA, **S**tratospheric **O**bservatory for **I**nfrared **A**stronomy. It will be installed in a Boeing 747 for operation in the stratosphere and will enable scientist to observe infrared sources inaccessible to ground based observatories. In opposition to space based telescopes free access to the science instrument (camera), demanded by the scientist, will be possible. The primary mirror diameter (aperture) will be 2.5 m and the focal length 49 m. Detailed information on the science objectives and capabilities of the observatory are given by Krabbe and Röser (1999).

To enable an unhampered entering of the infrared light, the primary mirror is situated in a cavity of the telescope directly exposed to the outside air (fig. 1). A bulkhead separates the cabin from the cavity and supports the telescope. The fundamental idea of the design is the bearing of the telescope in its centre of mass for insulation from aircraft rotational excursions. The attitude control loop, which is in the focus of this paper, is required for the stabilization of the telescopes inertial attitude. It consists of a gyro, sensing the inertial attitude of the telescope, a torque drive and the controller.

The extreme environmental conditions occurring in the aircraft are not comparable to earthbound or space telescopes. Particularly the exposure of the telescope to the outside flow in the cavity during operation leads to a strong excitation of motions and vibrations of the telescope. On the other hand the telescope is required to provide a high image stability of 1 arcsec RMS. This corresponds to an image motion of less than 250 μm on the focal plane. Magnified by the optics, motions and deformations of the telescope structure in the range of a few μm are sufficient to exceed this limit. For details on modelling and simulation of the image stability see Schönhoff *et al.* (2000a).

Therefore the precise attitude control of the telescope is an important requirement for image stability. In this paper the μ-synthesis method is applied to the problem in order to evaluate the limit of performance during the conceptual design.

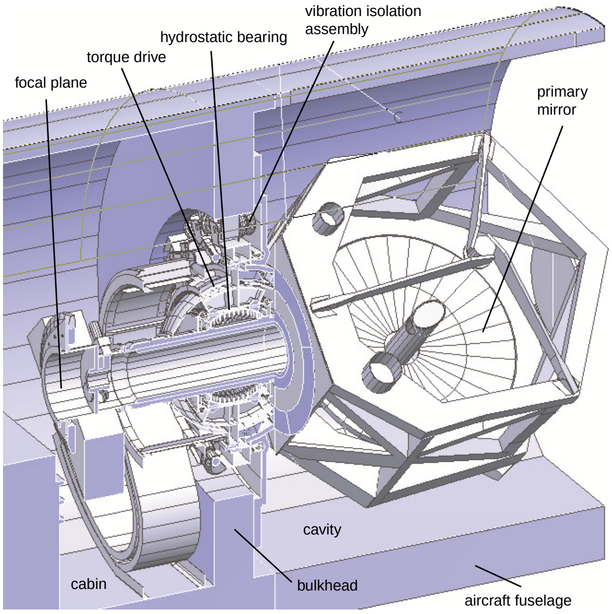

Figure 1: Scheme of the telescope

1.2 Problem formulation

The aim to minimize the RMS value of the image motion in the presence of aerodynamic disturbances originally is a H_2-synthesis problem. But for two reasons a H_2-minimization can not be performed: A model of the aerodynamic disturbance is required for this approach. But because the aerodynamic disturbance enters the structure distributed over the surface, a disturbance model is hard to derive, even though time histories from 56 pressure sensors exist, that are captured in a wind tunnel test of a scaled telescope model and are used for image motion simulation (Schönhoff *et al.*, 2000a). The second reason is that H_2-synthesis techniques do not address robustness issues sufficiently at this time. But robustness is an important prerequisite for the successful application. μ-synthesis is so far the only established synthesis technique, that guarantees robust performance. Unfortunately the performance optimization is based on the H_∞-criterion.

Abstaining from H_2-minimization one still would like to minimize the disturbance independent “compliance” of the image motion to an aerodynamic disturbance input similar to Knospe *et al.* (1997). Since the disturbance is not entering at a single point, this is not possible as well. For this reason only the controls (torque drive) and measurements (gyro) are evaluated. The main objective becomes the minimization of the transfer function $\boldsymbol{S}(j\omega)\boldsymbol{G}(j\omega)$ of the closed loop. This is the “compliance” of the attitude measured by the gyro to a virtual torque like disturbance applied at the torque drives location. For a flexible structure this is not exactly the same as the minimization aim mentioned before, but as long as mainly rigid-body rotation is controlled this is a a practicable approach to minimize the image motion.

1.3 Optimal and robust controller synthesis

Robust control design methods, first of all the μ-synthesis, have a great potential to industrial application. They meet a lot of industrial needs like MIMO-design, consideration of complex plant dynamics, inclusion of uncertainties, closed loop orientation, optimization and design formalism. They have already shown their capabilities in scientific applications (Steinbuch *et al.* 1998, Van den Braembussche, 1998, Knospe *et al.* 1997). Since many steps and skills like plant modelling, modelling of uncertainties, plant order reduction, selection of weighting functions, controller order reduction and discretization are required and numerical difficulties from large scaled systems are to overcome for a successful application, robust control has not found its way to industrial application yet. It is the aim of this paper to contribute to robust controls way towards application.

2 Modelling

The mechanical structure of the telescope is made of carbon fibre and weights 16000 kg for the most part from the primary mirror and the counter weight. Its first bending mode is found at 22.6 Hz. The model of the mechanical structure is the main part of the plant model. Since the telescope is currently under design and has not been constructed, a finite element (FE) model is the best choice to obtain a precise description of the structural dynamic to be expected. The FE-model constructed by MAN Technologie shows more than 100000 DOFs. It was reduced and imported to Matlab in modal representation with 200 states (Schönhoff *et al.*, 2000b). This model serves as a evaluation model in image motion simulation (Schönhoff *et al.*, 2000a).

The torque drive consists of 16 spherical elements, arranged in a manner to produce torques in all three axes. Each element is a self commutated three phase synchronous motor with permanent magnet excitation. Because the bandwidth of the current control loop is larger than 500 Hz, the dynamic of the torque drive is neglected in the model. For the measurement of the telescopes inertial attitude the telescope is equipped with a fibre optic gyro. The gyro is placed as close to the (non-lumped) torque drive as possible. Its limited bandwidth of approximately 80 Hz is considered in the model.

With regard to the discrete time realization a time delay of one sampling step for computation of the controller and 0.5 sampling steps for the zero order hold of the D/A-conversion is considered, and approximated by Pade all passes.

3 Performance specification

Specifying the performance requirements for H_∞-minimization means bounding the transfer functions of the closed loop. It is often stated that this is a non trivial task, neither in terms of the aspired H_2-performance nor in terms of reasonable time response of the closed loop. To formulate the specifications a proper a insight in this transfer functions is required.

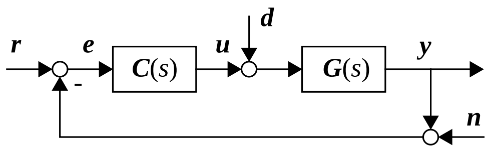

Figure 2: Closed control loop

Fig. 2 depicts the control loop, where ***y*** is the gyro attitude measurement, ***r*** the reference command, ***e*** the attitude error, ***u*** the current command to the torque drive, ***d*** the assumed disturbance and ***n*** the sensor noise. Each of this variables consist of three components for the 3 rotational DOFs to be controlled. The transfer function matrix

$$\begin{bmatrix} \boldsymbol{y}(s) \\ \boldsymbol{e}(s) \\ \boldsymbol{u}(s) \end{bmatrix} = \begin{bmatrix} \boldsymbol{T}(s) & \boldsymbol{S}(s)\boldsymbol{G}(s) & -\boldsymbol{T}(s) \\ \boldsymbol{S}(s) & -\boldsymbol{S}(s)\boldsymbol{G}(s) & -\boldsymbol{S}(s) \\ \boldsymbol{C}(s)\boldsymbol{S}(s) & -\boldsymbol{T}_i(s) & -\boldsymbol{C}(s)\boldsymbol{S}(s) \end{bmatrix} \begin{bmatrix} \boldsymbol{r}(s) \\ \boldsymbol{d}(s) \\ \boldsymbol{n}(s) \end{bmatrix} \qquad (1)$$

gives the relation between the inputs and outputs of the closed loop.

The minimization of the transfer function $\boldsymbol{S}(j\omega)\boldsymbol{G}(j\omega)$ is the main objective. It can be viewed as the “compliance” of the gyro attitude ***y*** to the virtual torque like disturbance ***d*** acting at the same location as the torque drive. A bound is put on the maximum value of this function in the rigid-body frequency range (Fig. 3). This bound determines the proportional action of the controller. The bound is levelled off first order to lower frequencies, which forces the controller to show integral action. For the flexible modes frequency range the bound is raised, because no controller action is desired in this range as long as the flexible modes keep stable. The actuator effort is described by $\boldsymbol{C}(j\omega)\boldsymbol{S}(j\omega)$. Even though economizing the control effort is not intended in this application, $\boldsymbol{C}(j\omega)\boldsymbol{S}(j\omega)$ has to be limited for two reasons: First $(\boldsymbol{C}(j\omega)\boldsymbol{S}(j\omega))^{-1}$ determines the robustness to additive uncertainties of the plant and is aspired to be high at high frequencies. Second it determines the shape of $\boldsymbol{C}(j\omega)$ at high frequencies, because $\lim_{\omega \to \infty} \boldsymbol{S}(j\omega) = 1$. A low pass characteristic of $\boldsymbol{C}(j\omega)$ rejects sensor noise and is extremely advan-

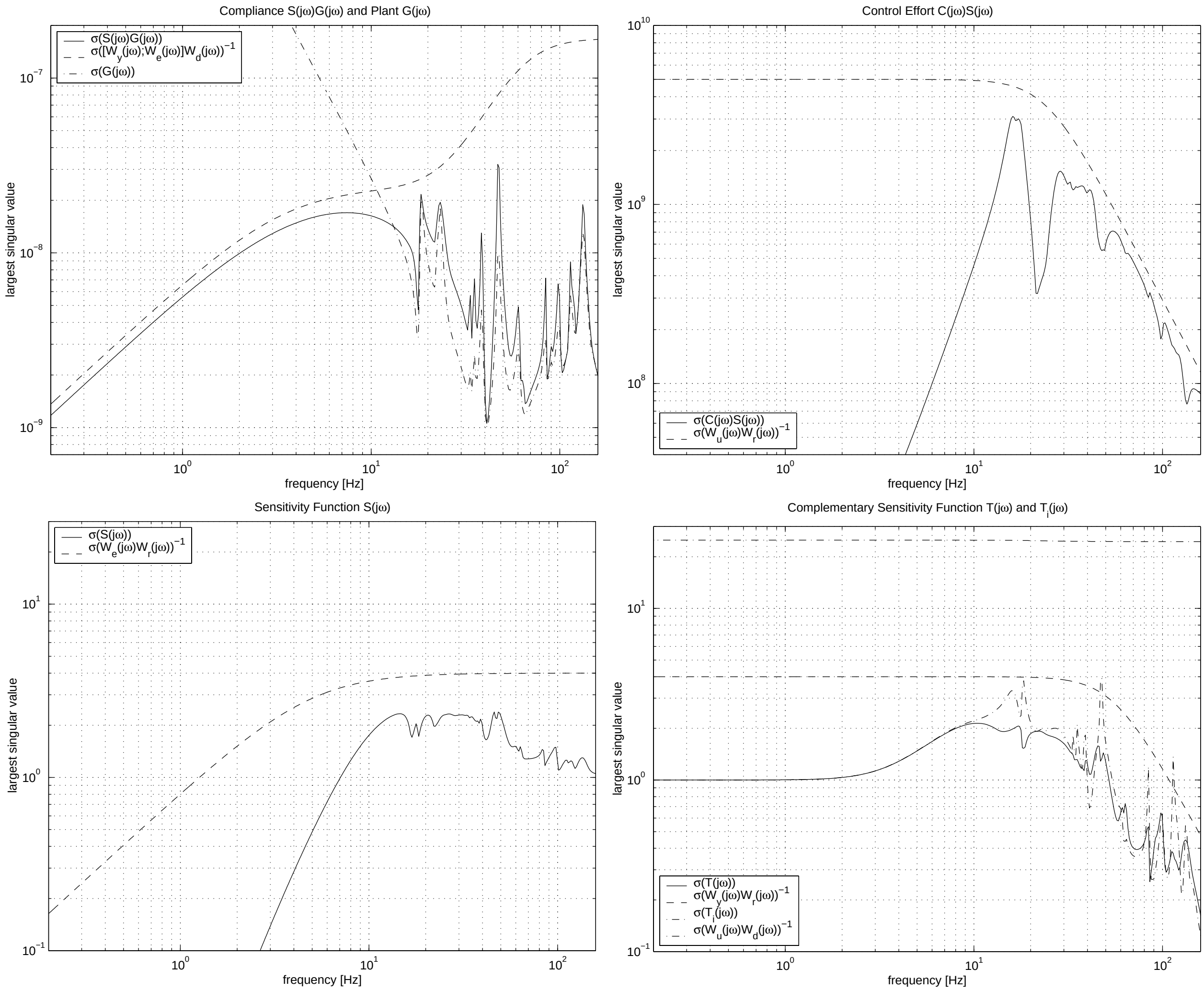

Figure 3: Transfer functions of the closed loop for the final μ-synthesis controller and their bounds

tageous for controller order reduction and discrete time implementation. A second order low pass bound was chosen.

Even though bounding of $\boldsymbol{S}(j\omega)\boldsymbol{G}(j\omega)$ and $\boldsymbol{C}(j\omega)\boldsymbol{S}(j\omega)$ already is sufficient to set up the optimization problem, limiting the sensitivity function $\boldsymbol{S}(j\omega)$ and the complementary sensitivity function $\boldsymbol{T}(j\omega)$ additionally is very useful to obtain reasonable controllers. A sensitivity function $\boldsymbol{S}(j\omega) > 1$ indicates that the controller is amplifying the disturbances entering the system. Experience has shown that $\boldsymbol{S}(j\omega)$ should be limited to approximately 3.

For lightly damped flexible structures putting a strict bound on $\boldsymbol{C}(j\omega)\boldsymbol{S}(j\omega)$ will cause the resonances of $\boldsymbol{G}(j\omega)$ to appear in $\boldsymbol{T}(j\omega)$ with high peaks. The reason is that the all-pass property of the H_∞-solution that makes $\boldsymbol{CS}$ shape its bound exactly by pole-zero cancellation. As a result the resonances of $\boldsymbol{G}$ appear by $\boldsymbol{T} = \boldsymbol{SGC}$ in $\boldsymbol{T}$ (Van Den Braembussche, 1998). This is undesired in all three meanings of $\boldsymbol{T}(j\omega)$ resp. $\boldsymbol{T}_i(j\omega)$[1], the reference action, the actuator response to disturbance and the transmission of sensor noise to the controlled variable. Hence the bound on $\boldsymbol{C}(j\omega)\boldsymbol{S}(j\omega)$ is relaxed and a bound on $\boldsymbol{T}(j\omega)$ with second order low pass characteristic is introduced.

To realize this SG-CS-S-T weighting scheme the inputs $\boldsymbol{r}$ and $\boldsymbol{d}$ and the outputs $\boldsymbol{y}$, $\boldsymbol{e}$ and $\boldsymbol{u}$ were chosen and augmented with the corresponding weighting functions $\boldsymbol{W}_{r...u}$:

$$F_l(\boldsymbol{P}, \boldsymbol{C}) = \begin{bmatrix} \boldsymbol{W}_y\boldsymbol{T}\boldsymbol{W}_r & \boldsymbol{W}_y\boldsymbol{S}\boldsymbol{G}\boldsymbol{W}_d \\ \boldsymbol{W}_e\boldsymbol{S}\boldsymbol{W}_r & -\boldsymbol{W}_e\boldsymbol{S}\boldsymbol{G}\boldsymbol{W}_d \\ \boldsymbol{W}_u\boldsymbol{C}\boldsymbol{S}\boldsymbol{W}_r & -\boldsymbol{W}_u\boldsymbol{T}_i\boldsymbol{W}_d \end{bmatrix}. \quad (2)$$

The weighting functions were designed to realize the desired bounds, e.g. $\bar{\sigma}(\boldsymbol{CS}) < \bar{\sigma}(\boldsymbol{W}_u\boldsymbol{W}_r)^{-1}$, and so to arrive at the H_∞-criterions, for this example $\|\boldsymbol{W}_u\boldsymbol{C}\boldsymbol{S}\boldsymbol{W}_r\|_\infty < 1$.

To determine the gains and cut-off frequencies of the bounds, first the optimal control problem without uncertainties is considered: First the bound for the “compliance” $\boldsymbol{S}(j\omega)\boldsymbol{G}(j\omega)$ in the rigid-body frequency range and the one for the integral action is chosen based on the disturbance rejection requirements. The bound on $\boldsymbol{C}(j\omega)\boldsymbol{S}(j\omega)$ is set to 100 times the inverse of the bound on $\boldsymbol{S}(j\omega)\boldsymbol{G}(j\omega)$ and a reasonable initial cut-off frequency is chosen. The bound on $\boldsymbol{S}(j\omega)$ is set to 4. The bound on $\boldsymbol{T}(j\omega)$ is set in the same manner as

1. Since $\boldsymbol{T}(j\omega) = \boldsymbol{SGC}$ but $\boldsymbol{T}_i(j\omega) = \boldsymbol{CSG}$, $\boldsymbol{T}_i(j\omega)$ is not exactly $\boldsymbol{T}(j\omega)$ if the plant $\boldsymbol{G}$ is not SISO.

the one on $\boldsymbol{S}(j\omega)$ and a fix relation of its cut-off frequency to the one $\boldsymbol{C}(j\omega)\boldsymbol{S}(j\omega)$, here 4, is chosen. The plant is augmented, the H_∞-synthesis is run and the cut-off frequency of the bound on $\boldsymbol{C}(j\omega)\boldsymbol{S}(j\omega)$ is adjusted iteratively until $\|F_l(\boldsymbol{P},\boldsymbol{C})\|_\infty < 1$ at least. To keep a margin for the uncertainties to be added in the next step, a value of about 0.95 was selected in this case. This scheme only depends on the key parameter "compliance". All other parameters follow from this or are fix.

All weights are chosen to have diagonal structure and equal diagonal elements are.

4 Plant order reduction

A precise plant model is a prerequisite for successful application of the controller. Derived from FE-analysis, this model is of high order. To perform the μ-synthesis it has to be reduced massively. But the question is, which degree of reduction is acceptable in order to obtain stability and performance of the full order plant model connected to the designed controller.

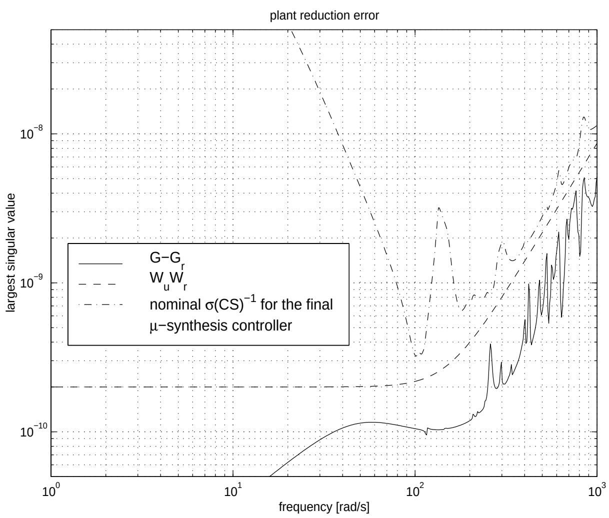

Figure 4: Plant reduction

The following two step procedure is used: Prior to the final design the plant model is reduced to a reasonable order and the weighting functions are determined based on the disturbance rejection requirement as explained before. The transfer function $\boldsymbol{CS}$ of this preliminary design gives the robustness to additive uncertainties by $\|\boldsymbol{CS}(\boldsymbol{G}-\hat{\boldsymbol{G}})\|_\infty < 1$. It marks off the admissible reduction error. Since $\bar{\sigma}(\boldsymbol{CS}) < \bar{\sigma}(\boldsymbol{W}_u\boldsymbol{W}_r)^{-1}$, it is straight forward to use the inverse of the weighting function of $\boldsymbol{CS}$ as a frequency weight for balanced truncation and aim for a reduction error less than one:

$$\|\boldsymbol{W}_r^{-1}(\boldsymbol{G}-\hat{\boldsymbol{G}})\boldsymbol{W}_u^{-1}\|_\infty < 1 \tag{3}$$

This approach allows to trade off between the desired disturbance rejection and the plant order. In this case the performance requirement was tightened until the order was up to 47. Fig. 4 shows the reduction error.

Subsequently the reduction error bound has to be considered as an additional uncertainty block $\boldsymbol{W}_u\boldsymbol{CS}\,\boldsymbol{W}_r$ in the final design to ensure the specified performance for the full order plant $\boldsymbol{G}$ connected to the controller designed with the reduced plant $\hat{\boldsymbol{G}}$.

In order to keep the augmented plant as simple as possible, this was not done in the presented design. Since $\boldsymbol{CS}$ is already bound in the performance block, the controller designed here will in any case stabilize the full order plant $\boldsymbol{G}$. In fact even the desired compliance was obtained.

5 Uncertainty modelling

Robustness to parameter variations of the plant and modelling errors is a requirement for practical control. Here the controller has to cope with

- changes in actuator gain (torque ripple) and actuator cross-talk of ±6 %,
- changes in the mass of the science instrument of ±32.5 kg (±5 %) and
- uncertainty in the modelling of the flexible structure.

Since the limitation of the complementary sensitivity function $\boldsymbol{T}(s)$ already ensures robust stability to multiplicative uncertainty of 25%, no additional uncertainty block is introduced for the actuator gain. To take the cross-talk into account, the off-diagonal elements of $\boldsymbol{W}_y\boldsymbol{W}_r$ were set to 0.06.

To model the change of the structural dynamics caused by the variation in the science instrument mass, it is not necessary to change the science instrument mass in the FE-model of the structure. Simply force inputs $\boldsymbol{f}_{SI}$ and acceleration outputs $\ddot{\boldsymbol{q}}_{SI}$ for the three translational DOFs of the science instrument are added to the FE-model and fed back by the mass variation m_δ. This results in a 3×3 repeated real uncertainty (Fig. 5).

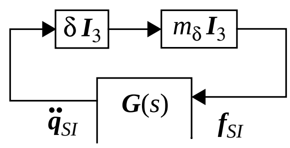

Figure 5: Parameter variation of the science instrument mass

Modelling errors in lightly damped flexible structures are typically small mismatches in the resonances. Since even small mismatches can cause large additive respectively multiplicative errors, they are modelled as parametric uncertainties in natural frequencies (Balas, Young, 1995). Assume that the system matrix $\boldsymbol{A}$ of the flexible mode part of the plant model is transformed by $\boldsymbol{T}$ to a real modal representation $\tilde{\boldsymbol{A}} = \boldsymbol{TAT}^{-1}$, where

$$\tilde{\boldsymbol{A}}_i = \begin{bmatrix} 0 & 1 \\ -(\omega_i(1+\delta_i))^2 & -2\xi_i\omega_i(1+\delta_i) \end{bmatrix} \tag{4}$$

is the 2×2 block for the ith mode on the diagonal of $\tilde{\boldsymbol{A}}$ and ω_i is the natural frequency of this mode with the relative uncertainty δ_i. The modal damping ξ_i is assumed to be constant, since it turned out to have no relevant influence on the controller design. Linearizing the term $(\omega_i(1+\delta_i))^2$ to

$\omega_i^2 + 2\omega_i^2\delta_i$, which is valid for the small uncertainties assumed, $\boldsymbol{A}_i$ can be rewritten as

$$\tilde{\boldsymbol{A}}_i \approx \begin{bmatrix} 0 & 1 \\ -\omega_i^2 & -2\xi_i\omega_i \end{bmatrix} + \begin{bmatrix} 0 \\ 1 \end{bmatrix} \delta_i \begin{bmatrix} -2\omega_i^2 & -2\xi_i\omega_i \end{bmatrix} \qquad (5)$$

and the uncertainty can be represented in a LFT with the output and input vectors $\tilde{\boldsymbol{C}}_{\delta_i} = [-2\omega_i^2 \ -2\xi_i\omega_i]$ and $\tilde{\boldsymbol{B}}_{\delta_i} = [0\ 1]^{\mathrm{T}}$ and a single real uncertainty δ_j. This reduces the number of uncertainties required per mode to one as compared to the commonly used 2×2 repeated blocks (e.g. Steinbuch *et al.*, 1998).

In order to keep the numerical condition of the original plant model, the plant model is not transformed to the modal coordinates; instead the uncertainty out- and input matrices $\tilde{\boldsymbol{C}}_\Delta$ and $\tilde{\boldsymbol{B}}_\Delta$, assembled form the vectors $\tilde{\boldsymbol{C}}_{\delta_i}$ and $\tilde{\boldsymbol{B}}_{\delta_i}$, are transformed back to the original coordinates: $\boldsymbol{C}_\Delta = \tilde{\boldsymbol{C}}_\Delta\boldsymbol{T}$ and $\boldsymbol{B}_\Delta = \boldsymbol{T}^{-1}\tilde{\boldsymbol{B}}_\Delta$. The numeric condition of the uncertainty out- and inputs is further improved by scaling the rows resp. columns of the of $\boldsymbol{C}_\Delta$ and $\boldsymbol{B}_\Delta$ to equal 2-norms.

In this application a uncertainty of $\pm1\,\%$ to all 17 modes contained in the reduced plant model is introduced with respect to later application.

6 μ-Synthesis

Having set up the controller design problem, the robust controller synthesis is carried out using the μ-synthesis. The augmented plant shows 68 states, a 9×6 unstructured performance block, 17 real scalar uncertainties in the natural frequencies and 3 real repeated uncertainties for the science instrument mass.

Since there is no direct solution to the μ-synthesis problem, three different iteration schemes are investigated. The first, the D-K-Iteration (Balas *et al.*, 1995), is commercially available and has become standard, but it is only capable to handle independent complex uncertainties. In this case, like in most applications, the parametric uncertainties are of real valued nature and also repeated uncertainties occur. Using the D-K-Iteration they have to be treated as complex uncertainties, which turns out be conservative. The later two approaches, the (D,G)-K-Iteration (Young, 1996) and the μ-K-Iteration (Tøffner-Clausen *et al.*, 1995) allow the designer to handle real and repeated uncertainties.

To perform the D-K-Iteration, measures had to be taken to avoid numerical problems: The flexible modes part of the model and the weighting functions are each balanced separately. Because the rigid-body modes part of the model is unstable, it was not possible to balance the entire augmented plant open loop. The uncertainty inputs and outputs are scaled as described in the section before in order to avoid ill conditioned D-scales. An initial controller was required to start the iteration. The H_∞-controller designed without uncertainties served for this purpose as well as a PID-controller with low gain, just designed for stabilization of the plant. Both were leading to the same result. For a accurate computation of μ the natural frequencies of the structure had to be included in the frequency grid. To reach convergence, the lowest tolerance on D-scale fitting had to be chosen and D-scales up to order 24 were required. The D-K-iteration converged in 9 steps. Extensive computation time of several hours was required. The order of the final controller was 186.

For this large scaled system the (D,G)-K iteration did not converge due to numerical problems. They occurred with the fitting and factoring the G-scale and with the H_∞-synthesis for the (D,G)-scaled plant. The μ-K-Iteration could not be finished, because the additional Γ-scaling reached orders larger 200, since it has to be applied to each uncertainty input.

After the first μ-synthesis controller was designed and the peak μ value was larger than 1, the performance specification on $\boldsymbol{S}(s)\boldsymbol{G}(s)$ was adjusted iteratively in order to reach a peak μ value near 1. The uncertainties were understood as fixed given values. The result is a controller archiving minimum robust compliance $\boldsymbol{S}(s)\boldsymbol{G}(s)$ for given uncertainties. Fig. 3 shows the closed loop transfer functions for the final controller and Fig. 6 the controller itself.

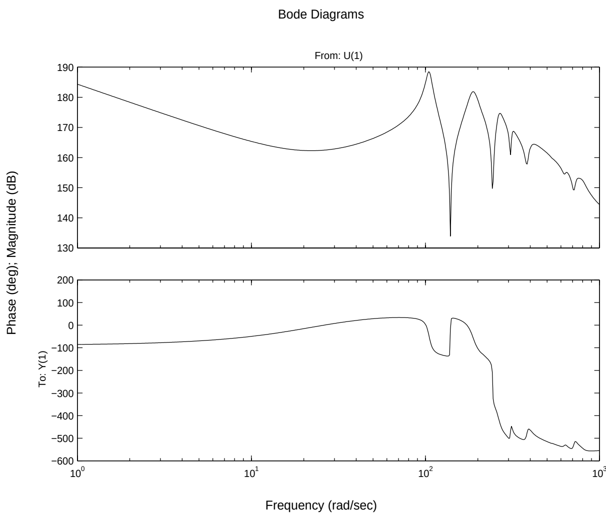

Figure 6: Exemplary frequency response $C_{(2,2)}$ of the final 3×3 MIMO controller form D-K-Iteration

7 Controller order reduction

The section model order reduction has shown the limits of model reduction in advance of the controller design. But as well as accurate modelling is demanded for reliable application, a low order of the controller is a prerequisite for economic realisation. Because the controller is of the order of the augmented plant plus the order of the D-scales added by the D-K-iteration, this leads to a contradiction that can only be solved by controller reduction.

Balanced truncation of the controller has become common practice after design. It aims an minimization of the maximum deviation $\|\boldsymbol{C}(s) - \hat{\boldsymbol{C}}(s)\|_\infty$ of the frequency response of the reduced controller $\hat{\boldsymbol{C}}(s)$ from the original controller $\boldsymbol{C}$ and offers significantly reduced controllers in most cases. But in order to reach the maximum degree of reduction, it is straight forward to address the preservation of robust performance

$$\min_{\hat{C}} \sup_{\omega} (\mu_\Delta(F_l(\boldsymbol{P}, \boldsymbol{C})) - \mu_\Delta(F_l(\boldsymbol{P}, \hat{\boldsymbol{C}}))) \quad (6)$$

directly. By replacing μ with its upper bound and using the D-scalings as in the D-K-iteration, $\mu_\Delta(F_l(\boldsymbol{P}, \boldsymbol{C}))$ becomes $\bar{\sigma}(\boldsymbol{D}_l F_l(\boldsymbol{P}, \boldsymbol{C}) \boldsymbol{D}_r^{-1})$ and the minimization problem can be formulated in terms of rational transfer functions (Rivera, Morari, 1992):

$$\min_{\hat{C}} \left\| \boldsymbol{D}_l F_l(\boldsymbol{P}, \boldsymbol{C}) \boldsymbol{D}_r^{-1} - \boldsymbol{D}_l F_l(\boldsymbol{P}, \hat{\boldsymbol{C}}) \boldsymbol{D}_r^{-1} \right\|_\infty . \quad (7)$$

This can directly be tackled by the frequency weighted balanced reduction in closed loop configuration (Wortelboer *et. al.*, 1999). It follows the standard balanced reduction procedure, but it is not using the Gramians of $\boldsymbol{C}$ itself. Instead the Gramians

$$\boldsymbol{P} = \begin{bmatrix} \boldsymbol{P}_{\boldsymbol{D}_l \boldsymbol{P} \boldsymbol{D}_r^{-1}} & \equiv \\ \equiv & \boldsymbol{P}_C \end{bmatrix} \text{ and } \boldsymbol{Q} = \begin{bmatrix} \boldsymbol{Q}_{\boldsymbol{D}_l \boldsymbol{P} \boldsymbol{D}_r^{-1}} & \equiv \\ \equiv & \boldsymbol{Q}_C \end{bmatrix} \quad (8)$$

of the augmented pant in closed loop, for the D-K-iteration this means $\boldsymbol{D}_l F_l(\boldsymbol{P}, \boldsymbol{C}) \boldsymbol{D}_r^{-1}$, are computed and their parts $\boldsymbol{P}_C$ and $\boldsymbol{Q}_C$ belonging to the controller states are used for balancing of $\boldsymbol{C}$.

A reduction from order 186 to 46 is reached without significant loss in performance in this application. Tab. 1 compares the robust performance for the of the unweighted and the in closed loop configuration reduced controller.

method	order r	$\sup(\mu_\Delta(F_l(\boldsymbol{P}, \hat{\boldsymbol{C}})))$
no reduction	186	0.98
$\boldsymbol{D}_l F_l(\boldsymbol{P}, \boldsymbol{C}) \boldsymbol{D}_r^{-1}$ -balanced truncation	46	1.00
balanced truncation	67	1.00
balanced truncation	46	1.28

Table 1: Robust performance of the closed loop

8 Conclusions

Since the operation of the telescope under the harsh environmental conditions in the aircraft makes the image stability a crucial issue, a μ-synthesis optimization of the attitude control loop is investigated. The design is based on a finite element model, that offers the most precise description of the structural dynamics of the telescope structure in the design phase. Modelling errors in the structural dynamics were considered in terms of uncertainties of the natural frequencies. Variations in the mass of the science instruments and torque ripple and cross-talk of the drive have also been taken into account as uncertainties. A weighting function scheme based on a few engineering parameters only was derived for performance specification. To obtain numerically reliable results, several measures had to be taken. Straight forward model and controller reduction with respect to robustness was performed. Finally a MIMO controller of order 46 was obtained. A significant increase of disturbance rejection compared to conventional designs was reached (Schönhoff *et al.*, 2000a). Robust controller design was brought into a continuous procedure, that faces the practical problems of application. Recent application results (Schönhoff *et al.*, 2000c) on the magnetic bearing control have shown the easy tansferability of this procedure and the operativeness of the μ-controllers.

Acknowledgements

We would like to thank the telescope manufacturer MAN Technologie AG, Gustavsburg, Germany for founding this work and the German space agency DLR for enabling it. We also thank Pepjin Wortelboer, who made the Wor-Toolbox available to perform the model and controller reduction, and Peter M. Young for making the (D,G)-K-Iteration software available. Thanks to the students Andreas Bootz, Ernst Prescha and Markus Ries for their commitment.

References

Balas, G.J.; Doyle, J.C.; Glover, K; Packard, A.K; Scmith, R. (1995): μ-*Analysis and Synthesis Toolbox.* MUSYN Inc., Mineapolis, MN and The Mathworks, Inc., MA.

Balas, G.J.; Young, P.M. (1995): Control design for variations in structural natural frequencies. *J. of Guidance, Control and Dynamics* **18**(2), 325-332.

Young, P.M. (1996): Controller design with real parametric uncertainty. *Int. J. of Control* **65**(3), 469-509.

Knospe, C.R.; Fittro, R.L.; Stephens, L.S. (1997): Control of a High Speed Machining Spindle via μ-Synthesis. *IEEE Conference on Control Applications*, Hartford, CT, 912-917.

Krabbe, A.; Röser, H.-P. (1999): SOFIA - Astronomy and Technology in the 21st Century. *Reviews of Modern Astronomy* **12**.

Rivera, D.E.; Morari, M. (1992): Plant and controller reduction problems for closed-loop performance. *IEEE Trans. on Automatic Control* **37**(3), 398-404.

Schönhoff, U.; Eisenträger, P.; Wandner, K.; Kärcher, H.; Nordmann, R. (2000a): End-to-end Simulation of the Image Stability for the Airborne Telescope SOFIA. *Astronomical Telescopes and Instrumentation* 2000, Munich, Germany.

Schönhoff, U.; Eisenträger, P.; Nordmann, R. (2000b): Reduction of finite element models of flexible structures for controller design and integrated modelling. Invited Paper to the *Int. Conf. on Noise and Vibration Engineering, ISMA25*, Leuven, Belgium, September 2000.

Schönhoff, U.; Luo, J.; Hilton, E.; Li, G.; Nordmann, R.; Allaire, P. (2000c): Implementation results of μ-synthesis control for an energy storage flywheel test rig. *7th Int. Symp. on Magnetic Bearings, ISMB-7*, Zurich, 317-322.

Steinbuch, M.; van Groos, P.J.M.; Schostra, G.; Wortelboer, P.M.R.; Bosgra, O.H. (1998): μ-Synthesis for a Compact Disc Player. *Int. J. of Robust and Nonlinear Control* **8**, 169-189.

Tøffner-Clausen, S.; Andersen, P.; Stoustrup, J.; Niemann, H.H. (1995): A New Approach to μ-Synthesis for Mixed Perturbation Sets. *3rd European Control Conference, ECC'95*, Rome, Italy, September 1995, 147-152.

Van Den Braembussche, P. (1998): *Robust motion control of high-performance machine tools with linear motors*. Ph.D. Thesis, Katholieke Universiteit Leuven, Leuven, Belgium.

Wortelboer, P.M.R.; Steinbuch, M.; Bosgra, O.H. (1999): Iterative model and controller reduction using closed-loop balancing, with an application to a compact disc mechanism. *Int. J. of Robust and Nonlinear Control* **9**(3), 123-142.